The Carboxyl-Terminal Region Common to Lamins A and C Contains a DNA Binding Domain†

Vérène Stierlé,‡ Joël Couprie,§ Cecilia Östlund,|| Isabelle Krimm,§ Sophie Zinn-Justin,§ Paul Hossenlopp,⊥ Howard J. Worman,|| Jean-Claude Courvalin,‡ and Isabelle Duband-Goulet*,‡

Département de Biologie Supramoléculaire et Cellulaire, Institut Jacques Monod-CNRS UMR 7592, Universités Paris 6/Paris 7, 2 place Jussieu, 75251 Paris cedex 05, France, Département d'Ingénierie et d'Etudes des Protéines, Bat. 152, CEA Saclay, 91191 Gif-sur-Yvette, France, Departments of Medicine and of Anatomy and Cell Biology, College of Physicians and Surgeons, Columbia University, New York, New York 10032, and Laboratoire de Minéralogie-Cristallographie Paris, CNRS UMR 7590, Universités Paris 6/Paris 7, 2 place Jussieu, 75251 Paris cedex 05, France

Received December 18, 2002

ABSTRACT: Lamins A and C are intermediate filament proteins which polymerize into the nucleus to form the nuclear lamina network. The lamina is apposed to the inner nuclear membrane and functions in tethering chromatin to the nuclear envelope and in maintaining nuclear shape. We have recently characterized a globular domain that adopts an immunoglobulin fold in the carboxyl-terminal tail common to lamins A and C. Using an electrophoretic mobility shift assay (EMSA), we show that a peptide containing this domain interacts *in vitro* with DNA after dimerization through a disulfide bond, but does not interact with the core particle or the dinucleosome. The covalent dimer binds a 30−40 bp DNA fragment with a micromolar affinity and no sequence specificity. Using nuclear magnetic resonance (NMR) and an EMSA, we observed that two peptide regions participate in the DNA binding: the unstructured amino-terminal part containing the nuclear localization signal and a large positively charged region centered around amino acid R482 at the surface of the immunoglobulin-like domain. Mutations R482Q and -W, which are responsible for Dunnigan-type partial lipodystrophy, lower the affinity of the peptide for DNA. We conclude that the carboxyl-terminal end of lamins A and C binds DNA and suggest that alterations in lamin−DNA interactions may play a role in the pathophysiology of some lamin-linked diseases.

The nuclear envelope surrounds and isolates chromatin from the cytoplasm. Chromatin is tightly attached to the nuclear envelope, the binding being mediated by transmembrane proteins of the inner nuclear membrane (reviewed in ref *1*) and by the nuclear lamina, which is apposed to the nucleoplasmic face of the inner nuclear membrane (reviewed in ref *2*).

A-type and B-type lamins, which are the building blocks of nuclear lamina, are members of the intermediate filament protein family and have similar primary structures (*3*, *4*). Both types of lamins polymerize in different ratios to form the filamentous meshwork of the nuclear lamina. In humans, A-type lamins are encoded by the *LMNA*[1] gene, which generates lamin A and lamin C by alternative RNA splicing (*5*). These proteins are identical for their first 566 amino acids, which encompass the amino-terminal head, the central dimerization rod domain, and most of the tail region. Lamins B1 and B2 are the two human B-type lamins. They are encoded by different genes and are expressed in all somatic cells. Several roles have been proposed for the peripheral nuclear lamina, including its involvement in nuclear structure and control of the perinuclear "silent" heterochromatin (*1*).

Recently, mutations in A-type lamins have been associated with several human genetic diseases, including autosomal dominant Emery-Dreifuss muscular dystrophy (EDMD) and Dunnigan-type familial partial lipodystrophy (FPLD) (reviewed in ref *6*). The role of lamins in the pathophysiology of these tissue specific diseases is intriguing since A-type lamins are expressed in almost all differentiated somatic cells. We recently analyzed the nuclear structure of fibroblasts from patients with FPLD and observed abnormally decondensed chromatin areas juxtaposed with disorganized lamina networks (*7*), suggesting that an alteration of lamina−chromatin interactions may play a role in the pathophysiology of the disease.

In this study, we investigated the *in vitro* binding to chromatin of a restricted domain of the carboxyl-terminal end of lamins A and C for the following reasons. First, in

† This work was supported by the Centre National de la Recherche Scientifique, l'Institut National de la Santé et de la Recherche Médicale, and la Fondation pour la Recherche Médicale, by grants from FEGEFLUC and l'Association Française des Myopathies to S.Z.-J., and by grants from the American Diabetes Association and Human Frontiers Science Program to H.J.W.

* To whom correspondence should be addressed. Phone: 33 1 44 27 77 63. Fax: 33 1 44 27 59 94. E-mail: dubandg@ijm.jussieu.fr.

‡ Institut Jacques Monod-CNRS UMR 7592, Universités Paris 6/Paris 7.

§ CEA Saclay.

|| Columbia University.

⊥ CNRS UMR 7590, Universités Paris 6/Paris 7.

[1] Abbreviations: AEBSF, 4-(2-aminoethyl)benzenesulfonyl fluoride; BSA, bovine serum albumin; DTT, dithiothreitol; ECL, enhanced chemiluminescence; EDMD, Emery-Dreifuss muscular dystrophy; EMSA, electrophoretic mobility shift assay; FPLD, Dunnigan-type familial partial lipodystrophy; GST, glutathione *S*-transferase; *LMNA*, lamin A/C gene; NLS, nuclear localization signal; NMR, nuclear magnetic resonance.

10.1021/bi020704g CCC: $25.00
Published on Web 04/09/2003

the widely acknowledged model of the assembly of intermediate filaments, the rod domains associate to form the core of the filaments while the carboxyl-terminal ends protrude outside of the filaments (*8*). Accordingly, previous studies have analyzed separately the chromatin interactions of the rod domain and of the carboxyl-terminal tail of lamins A and C (*9*, *10*), and the latter has been shown to mediate the interaction of lamins with chromatin (*10*, *11*). Second, the three-dimensional structure of the region of the carboxyl-terminal tail of lamins A and C located between amino acids 430 and 545 has been recently characterized both by NMR (*12*) and by crystallography (*13*), and shown to adopt an immunoglobulin (Ig) structure. In several families of transcription factors, Ig-like regions define the DNA binding domain (*14*). Here, we used an EMSA and NMR to investigate the chromatin binding of a peptide encompassing amino acids 411−553 of human lamins A and C, named here LA/C (411−553). It begins with an unstructured hydrophilic stretch of 19 residues containing the NLS with a ^{417}KKRKLE^{422} sequence (*4*), followed by the Ig fold domain and a downstream unstructured eight-amino acid residue stretch. Several mutations causing either EDMD or FPLD are located in this region. In particular, mutations linked to FPLD are clustered on a positively charged surface of the Ig fold domain with a "hot spot" at arginine 482 (*12*, *15*). We found that LA/C (411−553) dimers bind to DNA and that this binding is altered by mutations at this particular site.

EXPERIMENTAL PROCEDURES

DNA and Chromatin Preparations. The 357 bp fragment was obtained from a *Bam*HI digest of the plasmid pUC (357.4) (*16*). The 146 and 211 bp DNA fragments were obtained from the *Dra*I digest of the 357 bp fragment. The 67 bp DNA fragment was obtained from the *Dra*I and *Dpn*I double digest of the 357 bp fragment. The 16 bp oligonucleotide was synthesized as the self-complementary CGCGCGAATTCGCGCG base sequence by Genset (Paris, France). The mix of DNA fragments of approximately 400 bp was obtained by micrococcal nuclease digestion of rat liver chromatin, followed by gradient sedimentation, isolation of the dinucleosome fraction, and finally DNA extraction (∼360−420 bp) (*17*). Dephosphorylation of the DNA fragments and 5′-end labeling with [^{32}P]ATP and T4 polynucleotide kinase were performed according to standard protocols. For chromatin preparations, duck erythrocyte core histones were prepared as described previously (*18*), and then assembled on DNA fragments using the salt jump method with a final concentration of 100 mM in NaCl (*16*, *17*). Core particles and mononucleosomes were reconstituted on 146 and 211 bp DNA fragments, respectively, at a histone to DNA ratio of 0.4. Dinucleosomes were reconstituted on a 357 bp DNA fragment at a histone to DNA ratio of 1.

Lamin A Peptides. All cloning procedures were performed using standard methods (*19*). The plasmid encoding the GST fusion protein containing amino acids 411−553 of lamins A and C has been described previously (*12*). The plasmid encoding the GST fusion protein containing amino acids 423−553 of lamins A and C was obtained following the same procedure. Both plasmids were transformed into *Escherichia coli* strain BL21. Expression and purification of the GST−lamin fusion proteins were performed according to the manufacturer's instructions, using glutathione−Sepharose 4B beads (Amersham Pharmacia Biotech, Inc.). Purified chimeric proteins adsorbed on beads were digested with thrombin protease, generating soluble lamin fragments. For NMR studies, LA/C (411−553) and LA/C (423−553) peptides were dialyzed against 20 mM $NaHPO_4$ (pH 6.3) and lyophilized. For DNA binding experiments, the thrombin cleavage was performed in 10 mM Tris-HCl (pH 8.0), 1 mM EDTA, 100 mM NaCl, and 0.1% Triton X-100. The concentration of LA/C (411−553) was measured by the BCA protein assay (Pierce, Perbio Science).

Lamin A/C mutants R482Q and -W were generated in the same manner as the wild-type fragment except that lamin A R482Q or R482W mutant DNA (*20*) was used as the template in the polymerase chain reaction template. Peptide LA/C (414−427) containing the NLS sequence (CSVTKKRKLESTESR) was prepared by Eurogentec (Seraing, Belgium). Peptides were solubilized in 2× sample buffer (*21*), in the presence or absence of 100 mM DTT, followed by heating at 95 °C for 5 min. Electrophoretic analysis of the peptides was performed on 12.5% SDS−polyacrylamide gels. Immunoblotting experiments were performed as previously described, using a polyclonal rabbit antibody directed against a peptide containing the NLS sequence of human lamins A and C (*22*).

Peptide−DNA Interactions and the EMSA. Peptides diluted at the indicated concentrations in medium A [10 mM Tris-HCl (pH 8.0), 1 mM EDTA, and 1 mM 4-(2-aminoethyl)-benzenesulfonyl fluoride] containing 100 mM NaCl and 0.1% Triton X-100 were incubated with radioactive DNA fragments or reconstituted nucleosomes, either at room temperature for 3 h or at 8 °C overnight. Modifications in the binding medium are indicated in the figure legends. Protein−DNA complexes were analyzed on 4 or 5% polyacrylamide gels at an acrylamide/bisacrylamide ratio of 29/1 (w/w), in 0.5× TGE [12.5 mM Tris-HCl (pH 8.4), 95 mM glycine, and 0.5 mM EDTA], as indicated in the figure legends. After a 1 h pre-electrophoresis, samples were loaded and resolved at 70 V, by a 1−2 h electrophoresis depending upon the size of the DNA. DNA retardation was detected by autoradiography of the dried polyacrylamide gel at −80 °C, using Biomax MR film (Kodak) and an intensifying screen.

For affinity measurements, peptide−DNA binding was performed overnight at 8 °C in medium A containing 100 mM NaCl and 0.1% Triton X-100. Complexes were resolved on a 4% polyacrylamide gel in 0.5× TGE. Dried polyacrylamide gels were exposed to a phosphor screen, and measurements of the radioactive signals were performed with a STORM 860 scanner (Amersham) using ImageQuant software (Molecular Dynamics, Inc.). Competition experiments were performed as described for affinity measurements. Increasing concentrations of unlabeled competitor DNAs (67, 30, and 16 bp DNA fragments) were incubated with 13.5 nM labeled 67 bp DNA fragment (61 μM in base pairs) in the presence of 0.44 μM LA/C (411−553). Quantification of the radioactive signals was performed as described above. Molarities of bound, free, and total DNA fragments (expressed in base pairs) were calculated, and the percentage of bound DNA (B/T) was plotted as a function of DNA base pair molar excess.

Peptide−DNA Interactions Followed by NMR. The uniformly ^{15}N-labeled lamin carboxyl-terminal domain was produced in minimum medium M9 containing 1 g/L $(^{15}NH_4)_2SO_4$ (Boehringer). All the NMR experiments were carried out at 303 K on a 600 MHz Bruker spectrometer using a triple-resonance probe equipped with triple-axis gradients. NMR samples contained ∼1 mM ^{15}N-labeled protein dissolved in 20 mM phosphate buffer (pH 6.3). Titration of a 16 bp DNA onto the lamin peptide was followed by recording a series of ^{1}H−^{15}N HSQC spectra while adding small volumes of concentrated DNA to the peptide sample (final peptide/DNA ratio of 1/6). These spectra were processed with NMRpipe (*23*). Measurement of the chemical shift variations during the titration was carried out using FELIX (Molecular Simulations).

RESULTS

Production and Purification of the Native and Mutated LA/C (411−553). The recombinant glutathione *S*-transferase (GST) fusion protein containing LA/C (411−553) was purified from bacterial extracts. The chimeric protein was cleaved with thrombin to remove the GST and yield a 143-amino acid peptide. The same peptides with the R482Q or R482W mutation were also produced, as was a shorter wild-type peptide (residues 423−553), which does not contain the NLS (Figure 1A). The peptides were resolved by denaturing electrophoresis under reducing conditions and migrated in a manner consistent with their molecular masses (Figure 1B, lanes 2 and 3). In the absence of a reducing agent, a minor dimerization of the peptides was observed (Figure 1B, lane 4), likely due to oxidation of cysteine 522, the only cysteine present in the peptide. This dimerization became prominent with time, for example, when peptides were left for 3 h in solution in the absence of DTT, but was not total (Figure 1B, lane 5).

LA/C (411−553) Binds to DNA. The interaction of LA/C (411−553) with a 357 bp linear DNA fragment was studied by electrophoresis in a 4% polyacrylamide gel. Figure 1C (left panel) shows that, at 100 mM NaCl, the DNA formed four complexes with the peptide as demonstrated by delayed migration compared to naked DNA (Figure 1C, compare lanes 1 and 2). Larger complexes were observed at higher peptide concentrations (Figure 1C, compare lanes 2 and 3). DNA−peptide complexes persisted in 150 mM NaCl with or without 5 mM $MgCl_2$ (Figure 1C, lanes 7 and 8).

The NLS Is Required for Stable Binding of LA/C (411−553) to DNA. To investigate the role in DNA binding of the basic KKRKLE motif present at the amino-terminal end of LA/C (411−553), we made a shorter LA/C (423−553) peptide from which this motif was deleted (see Figure 1A). Figure 1D (lanes 12−15, signals B1−B4) shows that LA/C (411−553) rapidly saturated the 146 bp DNA and formed discrete protein−DNA complexes, while LA/C (423−553) generated only a fast migrating smear (Figure 1D, lanes 8−10). When a peptide containing the NLS (residues 414−427) was incubated with the 146 bp DNA fragment (Figure 1D, lanes 2−5), no significant bandshift was observed. Thus, the unstructured NLS peptide and the globular Ig domain, which alone poorly bind DNA, cooperate in LA/C (411−553) to generate a stable interaction with DNA.

LA/C (411−553) Binds DNA as a Dimer. As the experiments described above were performed in the absence of

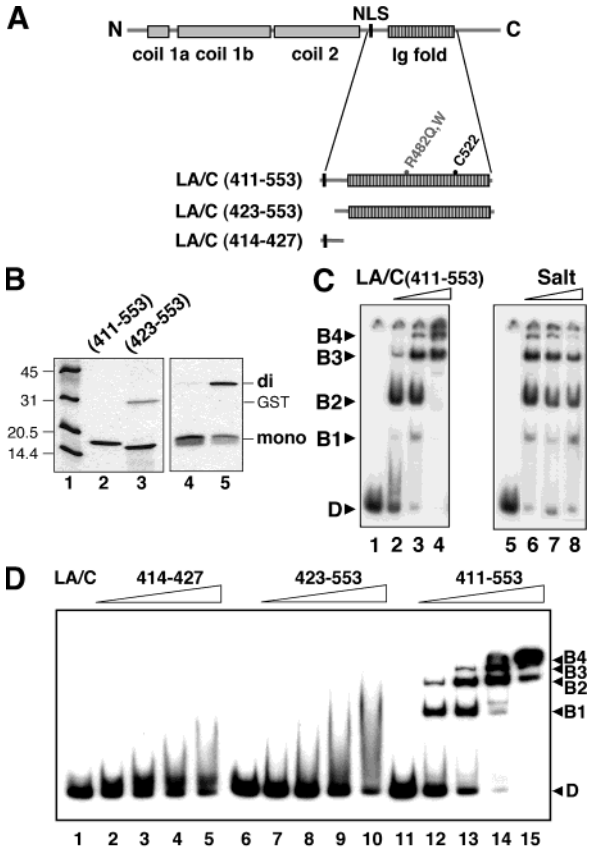

FIGURE 1: Peptide LA/C(411−553) binds to DNA. (A) Schematic representation of lamin A secondary structure. Gray boxes (coil 1a, coil 1b, and coil 2) indicate the rod domain, and NLS denotes the position of the nuclear localization signal. Downstream of the rod domain, the carboxyl-terminal end contains an Ig-like domain (dashed box). The limits of the peptides used in this study, LA/C (411−553), LA/C (423−553), and LA/C (414−427), are shown. The positions of the R482W and R482Q mutations and of the unique cysteine (C522) are indicated in gray and black, respectively. (B) SDS−polyacrylamide electrophoretic analysis of the peptides used in this study. Coomassie blue staining of gels in which LA/C (411−553) (lane 2) and LA/C (423−553) deleted for NLS (lane 3) were resolved under reducing conditions revealed signals of ∼18 and ∼16 kDa, respectively. Note a contamination of the latter preparation by cleaved GST. Under nonreducing conditions, a slight dimerization of LA/C (411−553) is observed (∼36 kDa, lane 4) which becomes prominent when the sample is left for 3 h at room temperature before analysis (lane 5). Lane 1 contained to molecular mass standards. (C) In the left panel, the 357 bp DNA fragment at a concentration of 11 nM in 100 mM NaCl was incubated in the presence of increasing concentrations of LA/C (411−553): 0.88 μM (lane 2), 1.76 μM (lane 3), and 3.52 μM (lane 4). Peptide−DNA complexes were named B1−B4 as a function of their decreasing mobilities. Lane 1 indicates the mobility of naked DNA (D). In the right panel, the interaction was performed as in lane 3, in the presence of different salt concentrations: 100 mM NaCl (lane 6), 150 mM NaCl (lane 7), and 150 mM NaCl and 5 mM $MgCl_2$ (lane 8). In both panels, electrophoresis was performed on 4% polyacrylamide gels. (D) The NLS peptide is necessary for stable LA/C (411−553) binding to DNA. LA/C (414−427) containing the NLS sequence (lanes 2−5), LA/C (423−553) (lanes 6−10), and LA/C (411−553) (lanes 12−15) were assembled on the 146 bp DNA. Concentrations of LA/C (414−427) and LA/C (423−553) peptides were 0.5 μM (lanes 2 and 7), 1 μM (lanes 3 and 8), 2 μM (lanes 4 and 9), and 4 μM (lanes 5 and 10). Concentrations of LA/C (411−553) were 0.44 μM (lane 12), 0.88 μM (lane 13), 1.76 μM (lane 14), and 3.52 μM (lane 15). Lanes 1, 6, and 11 show migration of naked DNA (D). Note that neither the NLS nor the 423−553 peptides alone were able to individually generate a bandshift, while a stable interaction with DNA is generated when both regions are present in LA/C (411−553) (lanes 12−15).

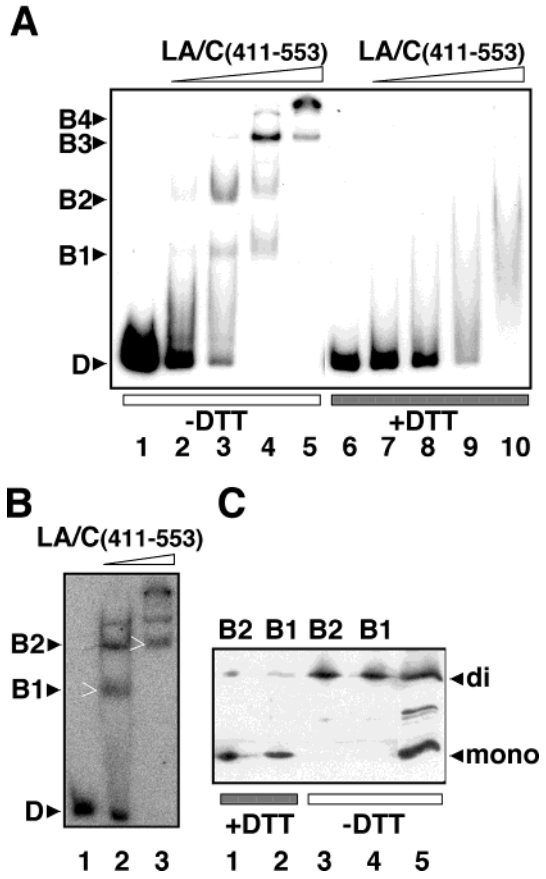

FIGURE 2: DNA interacts with a covalent dimer of LA/C (411−553). (A) The 357 bp DNA fragment was incubated with increasing concentrations of LA/C (411−553) as indicated in the legend of Figure 1D (lanes 12−15), either in the absence (lanes 1−5) or in the presence (lanes 6−10) of 1 mM DTT. Complexes were resolved on a 4% polyacrylamide gel. Note the absence of stable peptide−DNA interactions in the presence of DTT. (B) The 146 bp DNA fragment (52 nM) was incubated with a 30-fold (lane 2) or 60-fold (lane 3) molar excess of LA/C (411−553), and complexes were resolved on a 4% polyacrylamide gel. After autoradiography of the gel at room temperature, thin gel slices containing bands B1 and B2 (white arrowheads in lanes 2 and 3, respectively) were excised. Lane 1 refers to the migration of naked DNA (D). (C) One-half of each gel slice was incubated at 37 °C for 2 min in SDS sample buffer under nonreducing (−DTT) or reducing conditions (+DTT) as indicated. Both extracts were analyzed by denaturing electrophoresis on a 12.5% polyacrylamide gel, followed by immunoblotting using a polyclonal antibody against the NLS of lamin A/C. Lane 5 refers to the control LA/C (411−553) peptide analyzed under nonreducing conditions. Note that only dimers (lanes 3 and 4) were present in DNA−peptide complexes.

DTT, the binding of DNA to LA/C (411−553) may be dependent upon the formation of a covalent dimer of the peptide (see Figure 1B). This was investigated by incubating LA/C (411−553) with the 357 bp DNA fragment in the absence or presence of 1 mM DTT. The bandshifts observed in the absence of DTT (Figure 2A, lanes 2−5) were not observed in the presence of DTT (Figure 2A, lanes 7−10). Instead, a smear was observed at the highest peptide concentrations (Figure 2A, lanes 9 and 10), suggesting the presence of unstable DNA−protein interactions.

To confirm the existence of peptide dimers in the complexes, bands corresponding to complexes B1 and B2 (Figure 2B, white arrowheads) were isolated and then analyzed under reducing and nonreducing conditions on a SDS−polyacrylamide gel. Figure 2C (lanes 3 and 4) shows that, under nonreducing conditions, LA/C (411−553) that eluted from the complexes migrated exclusively as a dimer. As the peptide in solution was a mix of monomers and dimers (see Figure 1B, lane 5), this finding suggested that only dimers of the peptide were able to bind to DNA. All further experiments were performed in the absence of DTT.

LA/C (411−553) Dimers Bind a 30−40 bp DNA Site without Sequence Specificity. As the interaction of LA/C (411−553) with DNA generated complexes with different electrophoretic migrations, we examined whether these differences in shift were due to the independent binding to DNA of several dimers or of oligomers containing a higher number of LA/C (411−553) subunits. This was studied by comparing the binding of LA/C (411−553) to 146 or 67 bp DNA, respectively, the latter containing fewer potential protein binding sites. Complexes were analyzed on the same 4% gel. Figure 3A (lanes 6 and 7) shows that incubation with the 67 bp DNA fragment generated a major fast migrating complex (B1) and a minor slower migrating complex (B2) as opposed to the four complexes obtained with the 146 bp DNA (lanes 2−4). The decrease in the number of complexes, which parallels the shortening of DNA, suggests an independent binding of dimers to DNA. The binding of a maximum of four to five dimers of LA/C (411−553) on a 146 bp DNA and of two dimers on a 67 bp DNA predicts an ∼30 bp size for the binding site. When the migration of complexes was analyzed on a highly porous gel (3.2% polyacrylamide), nine bands were observed with the 357 bp DNA and six with the 146 bp DNA (data not shown), also predicting a 30−40 bp size for the DNA binding site. Because of the poor electrophoretic resolution of peptide−DNA complexes containing DNA of small sizes, the binding of LA/C (411−553) to <67 bp DNA was instead analyzed by competitive binding. We established an assay where a fixed amount of labeled 67 bp DNA bound to LA/C (411−553) was competitively inhibited with increasing concentrations of cold 67, 30, and 16 bp DNAs. Figure 3B shows that half-maximal competition was obtained with a 3.5-fold molar excess of base pairs with the 67 bp DNA fragment, with a 12-fold molar excess of base pairs with the 30 bp DNA fragment, and with a 48-fold molar excess of base pairs with the 16 bp DNA fragment. Thus, DNA of a size between 30 and 67 pb is a full competitor. These combined data suggest that the DNA binding site for LA/C (411−553) is around 30−40 bp in size.

To check for a putative DNA base composition that would preferentially bind to LA/C (411−553), the peptide was incubated with five DNA fragments of a similar size (between 344 and 357 bp) with different base compositions, and less than 10% sequence identity. Similar bandshifts were observed with DNA samples with a composition in AT varying from 37 to 57% (data not shown), showing that the binding was insensitive to the AT percentage. To check if this peptide binds to a specific DNA sequence, we generated from rat liver nuclei a DNA library of 360−420 bp fragments covering all sequences as exhaustively as possible. Although there was an apparent increase in the affinity of binding of the peptide for these DNA fragments (1.5-fold) compared with the affinity of binding to the 357 bp unique sequence, no strong signal was obtained at low peptide concentrations (Figure 3C, compare lanes 2 and 6), suggesting that LA/C

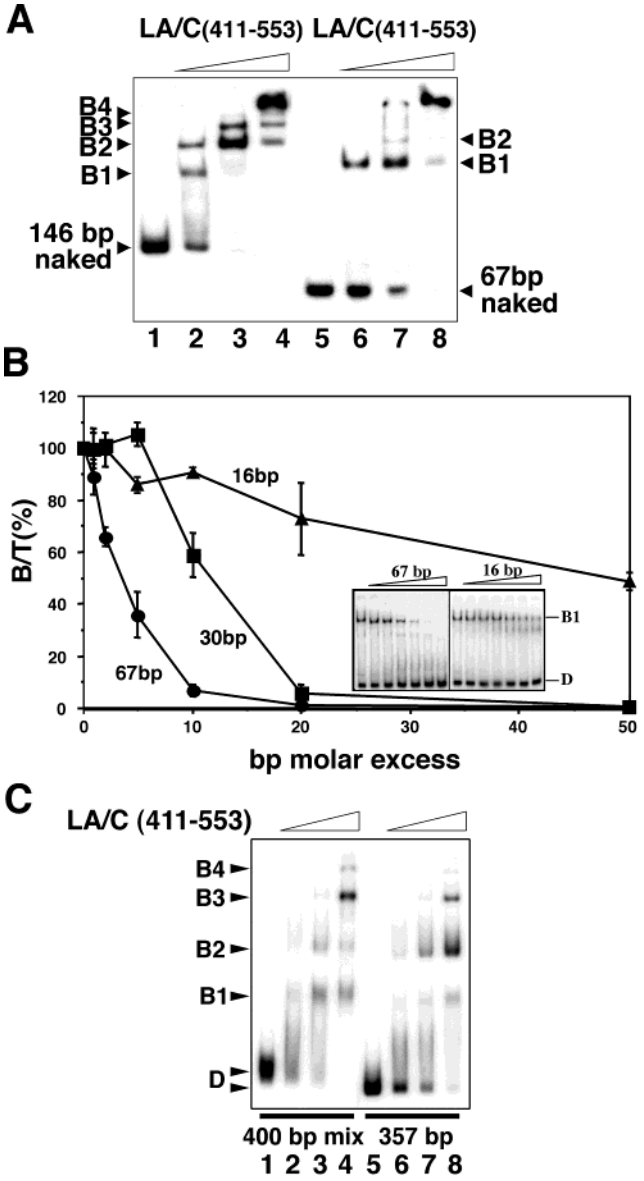

FIGURE 3: Dimers of LA/C(411−553) independently bind 30−40 bp DNA sites without sequence specificity. (A) Characterization of LA/C (411−553) oligomers in the DNA complexes. Increasing concentrations of LA/C (411−553), 0.44 μM (lanes 2 and 6), 0.88 μM (lanes 3 and 7), and 1.76 μM (lanes 4 and 8), were incubated with DNA fragments of either 146 bp (lanes 2−4) or 67 bp (lanes 6−8), at a concentration of 11 or 14 nM, respectively. Electrophoresis was performed on 4% polyacrylamide gels. The mobility of naked DNA fragments is indicated (lanes 1 and 5). Note that only complexes B1 and B2 were obtained with the 67 bp DNA fragment. (B) A mix of LA/C (411−553) (0.44 μM) and 67 bp labeled DNA (13.5 nM) was incubated with increasing concentrations of unlabeled 67, 30, and 16 bp DNA fragments. Complexes were resolved on a 4% polyacrylamide gel (left inset, competition with the 67 bp DNA; right inset, competition with the 16 bp DNA). Radioactive signals were scanned with a phosphoimager, and the percentage of labeled 67 bp fragment bound to the LA/C (411−553) peptide (B/T) was plotted as a function of the base pair concentration of the cold competitor. Calculations showed that 30 and 16 bp DNA fragments have 3.4- and 14-fold lower affinity for LA/C (411−553) than the 67 bp fragment, respectively. (C) LA/C (411−553) at increasing concentrations (as in panel A) was incubated with ~400 bp DNA fragments from a rat DNA library (lanes 1−4) or with the 357 bp DNA (lanes 5−8). Similar amounts of B1−B4 complexes were formed at similar peptide concentrations, showing that binding of LA/C(411−553) to DNA is sequence-independent. Lanes 1 and 5 refer to naked DNA migration (D).

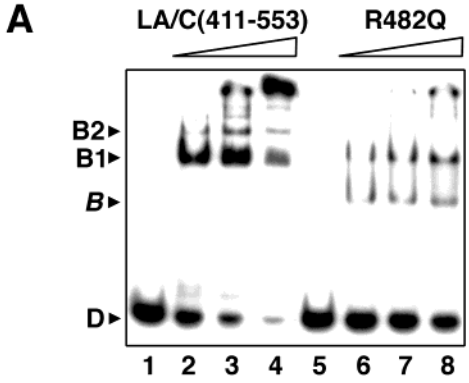

B

peptide	*kD*
native	
LA/C(411-553)	0.42 μM ± 0.1
mutants	
R482Q	2.19 μM ± 0.6
R482W	2.95 μM ± 0.7

FIGURE 4: Binding of LA/C (411−553) to DNA is altered by mutations that cause FPLD. (A) Increasing concentrations of LA/C (411−553), either wild-type (left panel) or mutated (right panel), were incubated with the 67 bp DNA fragment under conditions similar to those described in the legend of Figure 3A. The mobility of naked DNA (D) and that of peptide−DNA complexes B1, B2, and *B* are indicated. Lanes 1 and 5 refer to migration of DNA alone. Note the difference in complex mobilities as well as in the intensities of the signals between the native and R482Q mutant peptide. (B) Affinity measurement. Free and peptide-bound DNA signals detected at the lower peptide concentration (lanes 2 and 6) were quantified using a phosphorimager. The dissociation constant K_D was calculated using the equation $K_D = ([D] - [DP])([P] - [DP]/[DP])$, where [D] is the total DNA concentration, [P] the total peptide concentration, and [DP] the peptide−DNA complex concentration. The mean values obtained from three independent experiments are presented with the standard deviations.

(411−553) binds DNA with no apparent sequence specificity.

Mutations in LA/C (411−553) Diminish Its DNA Binding Affinity. FPLD is a disease caused by mutations in the *LMNA* gene, with a hot spot at arginine 482 (90% of cases). This amino acid is located in a large positively charged region at the surface of the Ig-like domain, which may constitute a DNA binding region (*12*). We produced LA/C (411−553) bearing the R482Q or R482W mutation and studied the interaction of the two mutant peptides with the labeled 67 bp DNA fragment. Figure 4A shows that saturation of DNA (14 nM) was almost complete at a concentration of 1.76 μM for the wild-type peptide (lane 4), while it was not achieved for the R482Q mutant (lane 8). Estimated K_D values were 0.42 μM for the wild-type peptide and 2.19 and 2.95 μM for R482Q and R482W mutant peptides, respectively (Figure 4B). Thus, the two mutations at R482 cause a 5-fold decrease in the affinity of LA/C (411−553) for DNA. In addition to the changes in affinity, qualitative differences in the interactions were also observed. Figure 4A shows that the B2 complex was not formed with the R482Q mutant, while a faster migrating complex was present (Figure 4A, lanes 6−8, signal B). Similar data were obtained with the R482W mutant (data not shown).

LA/C (411−553) Does Not Bind Core Particles or Dinucleosomes. We further analyzed the binding of LA/C (411−553) to reconstituted mononucleosomes and dinucleosomes (Figure 5). Core particles (CP, nucleosomes without linkers) were reconstituted using a 146 bp DNA and purified core histones. As shown in Figure 5A (lane 1), the preparation was a mix of core particles migrating as a single band and naked DNA. In the presence of increasing concentrations, LA/C (411−553) selectively bound to naked DNA (Figure 5A, lanes 2−4). The migration of the complexes was similar to that of the complexes obtained by incubation of LA/C (411−553) with the 146 bp DNA alone (Figure 2A, right panel, lanes 6−8). Thus, there was no supershift due to the formation of a core particle−LA/C (411−553) complex.

When nucleosomes were reconstituted with a 65 bp longer DNA fragment (211 bp), two bands corresponding to mononucleosomes (as seen by micrococcal digestion, data not shown) with linker DNA were formed (see the scheme in Figure 5B). When LA/C (411−553) was incubated at increasing concentrations with this chromatin preparation, complexes first formed with naked DNA (Figure 5B, lane 2, complexes B1 and B2) and then with N nucleosomes (Figure 5B, lanes 3 and 4, complexes $B1_N$ and $B2_N$). As N nucleosomes contain linker DNA that is absent from core particles, these data suggest that the peptide preferentially binds this linker.

Finally, nucleosomes were reconstituted on the 357 bp DNA in the presence of increasing concentrations of the histone octamer (Figure 5C, lanes 1−3). At a histone/DNA ratio of 1, a dinucleosome preparation free of DNA and mononucleosomes was obtained (Figure 5C, lane 3, scheme), which was incubated in the presence of increasing concentrations of LA/C (411−553) (Figure 5C, middle panel, lanes 4−6). No shift of the dinucleosomes occurred, while naked DNA migration was shifted under the same experimental conditions (Figure 5C, lanes 8−10). These data show that LA/C (411−553) does not bind core particles, or dinucleosomes, but binds the DNA linker in mononucleosomes.

NMR Identifies Two Distinct DNA Binding Motifs in LA/C (411−553). We used heteronuclear NMR to map the DNA binding sites on LA/C (411−553). We added various amounts of a palindromic DNA of 16 bp to an LA/C (411−553) sample, and by recording $^1H-^{15}N$ HSQC spectra, we identified which residues had a chemical environment perturbed by the addition of DNA. The size of the 16 bp DNA fragment was not optimal for the binding to LA/C (411−553) in EMSA studies (see Figure 3B), but allowed for an analysis of the DNA−peptide complex by NMR. Figure 6 shows the superposition of the $^1H-^{15}N$ HSQC spectra of free LA/C (411−553) and LA/C (411−553) with a saturating amount of DNA. A progressive displacement of several cross-peaks was observed throughout the titration. Fitting these displacements to a titration curve revealed that the lamin fragment binds to the oligonucleotide with an affinity of 0.65 ± 0.05 mM. Identification of the cross-peaks shifting during the titration allowed us to identify the protein regions involved in DNA binding (Figure 7A). The parts of LA/C (411−553) perturbed by the addition of DNA were the amino-terminal unstructured region preceding the Ig-like domain, the end of the B−C loop, the C′−E loop, the region around the β7 strand specific to the lamin Ig fold, the F−G loop, and the carboxyl-terminal unstructured residues fol-

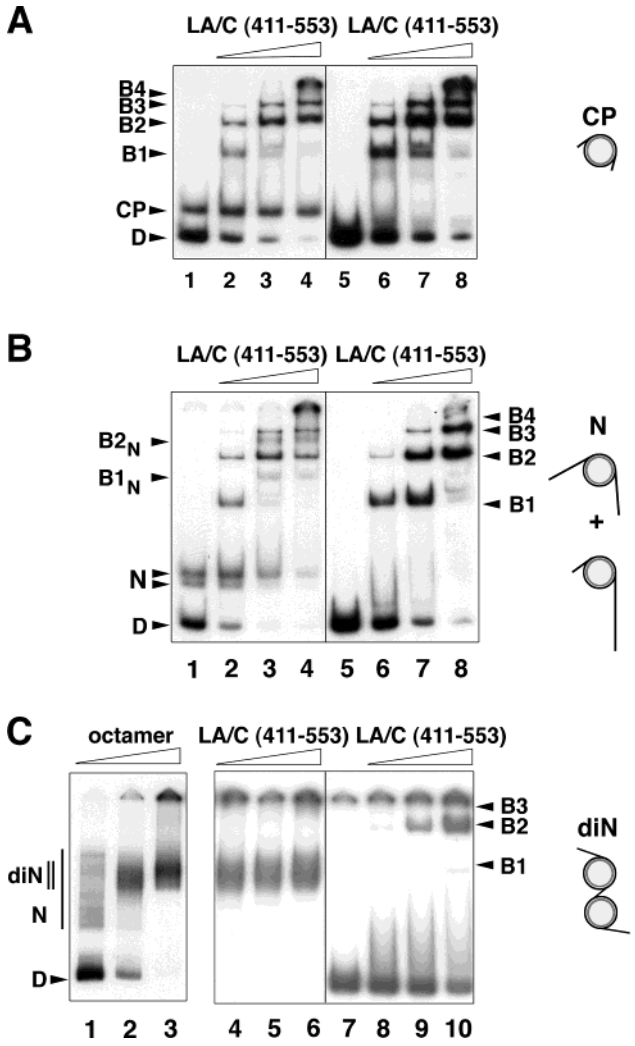

FIGURE 5: LA/C (411−553) binds naked DNA and linker DNA but does not bind the core particle or the dinucleosome. (A) Nucleosomes without linker DNA (core particles) were reconstituted on a 146 bp DNA fragment (see the scheme, CP) and then resolved on a 4% gel (lane 1). D and CP refer to DNA and core particle mobilities, respectively. The same chromatin preparation was incubated with increasing concentrations of LA/C (411−553), as in Figure 3A. A control experiment was performed under similar conditions with DNA alone (lanes 5−8). Note that, in the two panels, LA/C (411−553) formed similar complexes with naked DNA. Lane 5 refers to the migration of naked DNA. (B) Nucleosomes with linker DNA were reconstituted on a 211 bp DNA fragment and then resolved on a 4% gel (lane 1). D refers to DNA and N to nucleosomes (see the scheme, N). In lanes 2−4, the nucleosome preparation was incubated with increasing concentrations of LA/C (411−553), as indicated for panel A. A control experiment was performed under similar conditions with DNA alone (lanes 5−8). Note the presence of two additional signals, $B1_N$ and $B2_N$ in lanes 3 and 4, which correspond to the selective binding of the peptide to linker DNA present in N. (C) Nucleosomes were reconstituted on a 357 bp DNA fragment at increasing histone octamer/DNA ratios and then analyzed on a 5% gel (left panel, lanes 1−3). Ratios were 0.65 (lane 1), 0.8 (lane 2), and 1 (lane 3). Mononucleosomes (N) and dinucleosomes (diN) were progressively formed, the latter being predominant in lane 3. D refers to naked DNA. In the middle panel (lanes 4−6), dinucleosomes reconstituted under the conditions of lane 3 were incubated with increasing concentrations of LA/C (411−553), identical to that used for panel A. In the right panel, the peptide at similar concentrations was incubated with the 357 bp DNA alone (lanes 8−10). Lane 7 shows the migration of the naked DNA. Note the absence of a dinucleosome shift, compared to the shift of naked DNA.

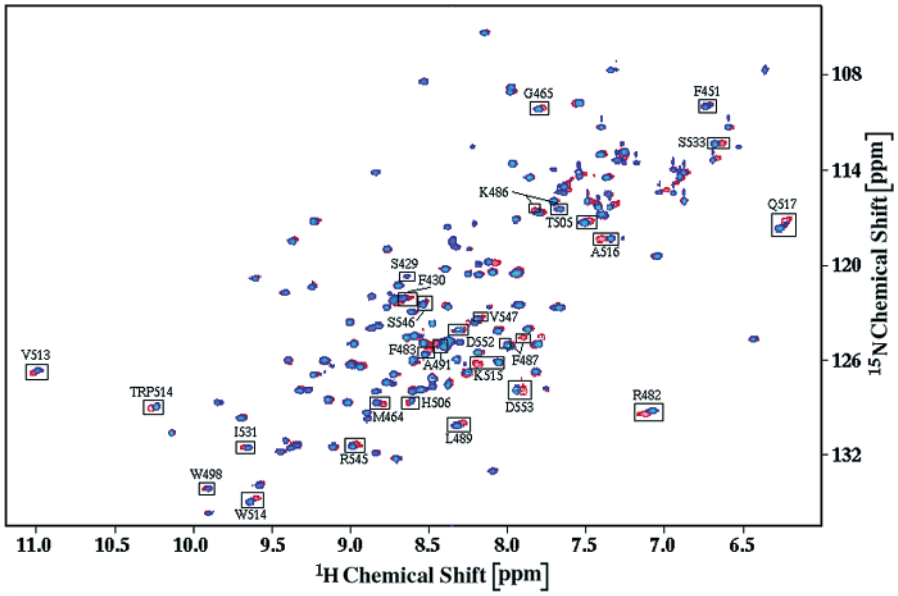

FIGURE 6: Superposition of the ^{1}H−^{15}N HSQC spectra of free LA/C (411−553) and LA/C (411−553) in complex with DNA. The cross-peaks in blue correspond to the spectrum of the free protein, and the cross-peaks in red correspond to the spectrum of the peptide−DNA complex (1/6 ratio). The peak shifts caused by the addition of DNA to the protein sample are boxed and annotated.

lowing the Ig fold (Figure 7A). The most important chemical shift variations ($\Delta\delta_H + 0.1\Delta\delta > 0.05$ ppm) were observed for the backbone amide bonds of Glu 422 and Ser 429 at the amino terminus, Arg 482, Phe 483, Lys 486, and Phe 487 in the C′−E loop, and Trp 514, Lys 515, Ala 516, and Gln 517 in the E−F loop, as well as for the side chain amines of Asn 466 (close to the C′−E loop) and Gln 517 (in the E−F loop). Lys 417, Lys 418, Arg 419, and Lys 420 from the NLS sequence could not be assigned, and thus, their involvement in the DNA interface cannot be confirmed. However, it is clear that unstructured residues from the amino and carboxyl termini close to the NLS, as well as residues from the Ig-like domain, are involved in DNA binding (Figure 7A).

Most residues of the Ig-like domain exhibiting important chemical environment perturbations during the titration are conserved throughout the lamin family. In particular, in most lamin sequences, residues homologous to Arg 482, Lys 486, and Lys 515 of LA/C (411−553) are positively charged, Phe 483, Phe 487, and Trp 514 of LA/C (411−553) are replaced with aromatic amino acids, and a glutamine is found at position 517. These seven residues, as well as the less conserved Asn 466 and Ala 516, are all found in the same region of the Ig-like domain (Figure 7B), which was identified as a large positively charged surface in our previous structural analysis (*12*). Thus, LA/C (411−553) interacts with DNA both via a set of unstructured residues close to the NLS and via a conserved positively charged region at the surface of the Ig-like domain.

To understand the role played by the NLS in the binding of LA/C (411−553) to DNA, we have tested the interaction between the shorter LA/C (423−553) peptide and the palindromic DNA of 16 bp by NMR. No ^{1}H−^{15}N HSQC cross-peak displacements corresponding to $\Delta\delta_H + 0.1\Delta\delta_N > 0.05$ ppm could be observed in this case, showing that LA/C (423−553) has a significantly lower affinity for DNA than LA/C (411−553). The most important ^{1}H−^{15}N HSQC cross-peak displacements observed upon addition of DNA ($0.02 \text{ ppm} < \Delta\delta_H + 0.1\Delta\delta_N < 0.05$ ppm) were found for residues Asp 446 and Lys 450 in the A−B loop, Phe 483, Lys 486, and Leu 489 in the C′−E loop, and Lys 515, Gln 517, and Thr 519 in the E−F loop. These residues are all located in the Ig fold region already identified as interacting with DNA in LA/C (411−553). Thus, when the first 12 residues comprising the NLS are deleted, the affinity of the lamin peptide for DNA decreases, and only a weak binding mediated by the described positively charged region at the surface of the Ig-like domain is conserved.

The structural study of LA/C (411−553) confirmed that, in the presence of DTT, the lamin fragment is mainly monomeric (*12*). Recording a ^{1}H−^{15}N HSQC spectrum with or without DTT showed that the region around Cys 522 exhibits proton and nitrogen chemical shift modifications in parallel with changes in the reducing agent concentration. In particular, ^{1}H−^{15}N HSQC cross-peaks corresponding to Glu 447, Glu 448, and Gly 449 in the A−B loop and Trp 520, Gly 521, Cys 522, Gly 523, and Ser 525 in the E−F loop show a shift corresponding to a $\Delta\delta_H + 0.1\Delta\delta_N$ value higher than 0.05 ppm, suggesting that these residues are located at the interface between two monomers of lamins within the covalent dimer. Interestingly, in a model of two LA/C (411−553) monomers linked by a disulfide bridge involving Cys 522, when the monomers are "modelized" in an antiparallel position, residues 447−451 and 519−525 form the interface between the two monomers. In this model, the region formed by the amino and carboxyl termini of one monomer become contiguous to the E−F and C′−E loops of the other monomer, generating a continuous DNA binding surface (Figure 7B). This surface has a size consistent with the binding to an oligonucleotide of approximately 14 bp. Thus, two of these surfaces symmetrically juxtaposed in the dimer would be able to bind a DNA fragment of a size similar to that found by EMSA analysis.

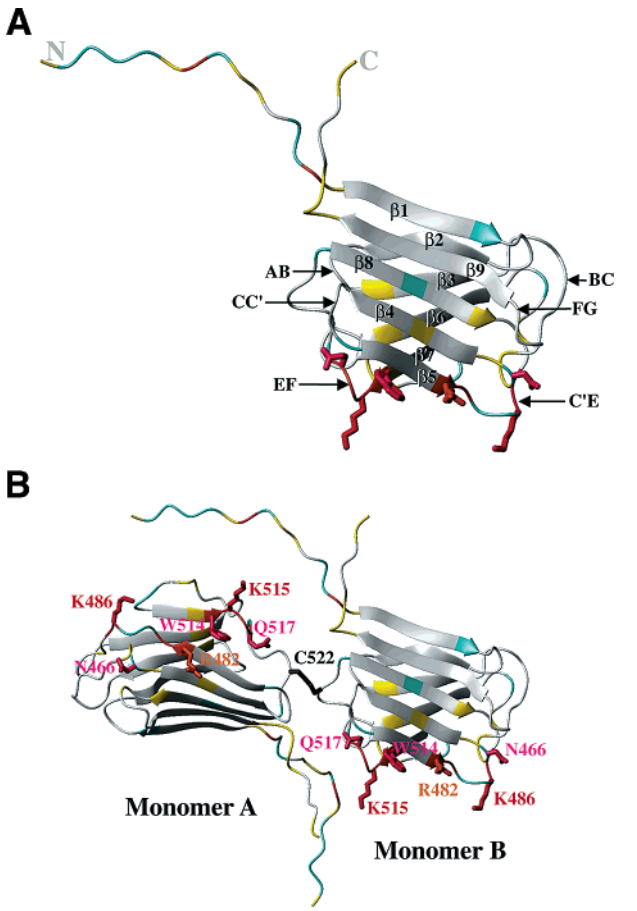

FIGURE 7: (A) Backbone structure of LA/C (411−553), as determined by NMR (*20*). Loops are annotated following the classical Ig fold nomenclature. β-Strands are labeled sequentially from β1 to β9. The unstructured amino- and carboxyl-terminal regions are arbitrarily positioned. The ribbon is colored as a function of the chemical shift variations exhibited by the backbone amide protons and nitrogens after addition of 6 equiv of DNA molecules: gray for $\Delta\delta_H + 0.1\Delta\delta_N$ values lower than 0.02 ppm and yellow and red for $\Delta\delta_H + 0.1\Delta\delta_N$ values higher than 0.02 and 0.05 ppm, respectively. Side chains are colored in red when their amine groups exhibit chemical shift variations such that $\Delta\delta_H + 0.1\Delta\delta_N$ values are higher than 0.05 ppm. The cyan ribbon corresponds to residues that could not be observed (lack of chemical shift assignment, superposition of the cross-peaks). The side chain of Arg 482 is displayed in green to indicate its position relative to the DNA binding site. (B) Model of a LA/C (411-553) covalent antiparallel dimer, in which the two distinct DNA binding surfaces displayed in panel A are contiguous. The color code of the protein ribbon is the same as in panel A. The disulfide bridge is colored black. The side chains shown to be involved in the interaction with DNA are labeled.

DISCUSSION

We have characterized the interactions between the Ig-like domain of the carboxyl-terminal region common to all A-type lamins and chromatin. We showed using an EMSA that a covalent dimer of a peptide containing this domain binds nonspecific DNA sequences with a micromolar affinity, but does not bind to core particles or to dinucleosomes. Using an EMSA, we also demonstrated that two regions of the lamin peptide participate in the DNA binding, the unstructured amino-terminal segment containing the NLS and the Ig-like domain, and that mutations in the latter causing FPLD decrease the affinity of the peptide for DNA. Although NMR analyses of the DNA−peptide interactions were performed with different DNA oligomers for technical reasons, consistent data were obtained, showing that the binding to DNA is mediated through the NLS and a positively charged surface of the Ig domain, which contains the amino acids mutated in FPLD. On the basis of the NMR data, we propose a model where two Ig fold domains of an opposite polarity form a dimer which binds to DNA.

Comparison with Previous Lamin−Chromatin Interaction Studies. Previous *in vitro* studies have shown that full-length or truncated A-type lamins can bind to naked DNA (*24*−*26*). Shoeman and Traub (*24*) found a low-affinity binding ($K_D \sim 0.35$ μM) of lamins A and C to a double-stranded oligonucleotide telomere sequence. Ludérus and co-workers (*26*) reported a stronger association ($K_D \sim 3.5$ nM) of vertebrate lamins A and C with the *Drosophila* histone matrix-associated region (MAR), although with a limited sequence specificity. However, as these studies were performed with full-length lamin proteins, they may have analyzed both DNA−lamin and lamin−lamin associations.

Complex chromatin substrates, such as chromosomes (*9*, *11*, *27*, *28*) and polynucleosomes (*10*, *11*), were also shown to bind A-type lamins. Höger and co-workers (*11*) found a binding site for reconstituted chromosomes in *Xenopus* lamin A, which was restricted to the extreme carboxyl-terminal end of the protein distal to the domain we have studied. Taniura and co-workers (*10*) have shown that the carboxyl-terminal tail of lamin C binds to polynucleosomes. They did not observe a direct binding of the lamin C tail to DNA, but instead characterized core histones as the component responsible for the interaction with chromatin. The divergent conclusions between the latter study and this study may be explained by the difference in the lengths of the lamin peptides which were analyzed, or/and by the different experimental procedures (solid phase assay vs EMSA).

Can the Covalent Dimerization of LA/C (411−553) at Cysteine 522 Exist in the Nuclear Lamina? In living cells, cytosol and nucleoplasm are under reducing conditions due to a large pool of reduced glutathione. However, the nucleus contains the thioredoxin/thioredoxin reductase enzymes that catalyze the oxido/reduction of thiols (*29*), and disulfide bonds have been observed in proteins from the nuclear matrix (*30*) and in surf clam oocyte lamins (*31*). Cysteine 522 was not buried in LA/C (411−553) or in the larger lamin C fragment (411−572) (data not shown); thus, a disulfide bridge at this site may exist *in vivo*. Molecular modelization favors its occurrence between antiparallel LA/C (411−553) peptides. In a dimer of lamins with parallel rod domains, the 42-amino acid loop (389−430) located between the rod and the Ig domains is long enough to allow the two Ig domains to adopt an antiparallel position. Alternatively, antiparallel Ig dimers may be formed by distant lamin molecules from antiparallel protofilaments of adjacent protofibrils (see Figure 11 in ref *2*). Finally, we do not exclude the possibility that in our *in vitro* experiments, disulfide bonds may have bridged Ig domains, which form noncovalent dimers either in the lamina or in the intranuclear pool of lamins (*32*, *33*).

Similarities with Other DNA Binding Proteins. Rudolph and Gergen (*14*) recently reviewed examples of Ig-like domains from transcription factors, which bind DNA after antiparallel dimerization. Several differences exist between the DNA binding mode of these transcription factors and

our model of lamin A and C−DNA interaction. (i) The DNA binding site for a lamin dimer (30−40 bp) is larger than that of transcription factors (<22 bp). (ii) While loops in transcription factors interact with palindromic DNA sequences in both sequence-dependent and -independent fashions, loops in LA/C (411−553) bind DNA only in a sequence-independent manner. (iii) K_D values for transcription factors vary from the picomolar to the nanomolar range, while they are in the micromolar range for LA/C (411−553). We suggest that, while Ig-like domains from transcription factors, which are regulatory proteins, bind a few DNA specific sites with high affinity, A-type lamins, which are structural proteins, bind multiple DNA sites without sequence specificity and with low affinity. The high number of DNA binding sites and their regular spacing could ensure a tight connection between the nuclear envelope and the chromatin. In addition, LA/C (411−553) could also interact with sequence specific DNA binding proteins, thus interfering with the expression of targeted genes in a cell-type specific manner, as shown for other proteins (*34*).

Several DNA binding proteins use an unstructured basic amino-terminal arm, in addition to a positively charged surface on a globular domain, to make contacts with DNA without sequence specificity. For example, dimeric Ku DNA repair protein binds to DNA in a sequence-independent fashion and with a high affinity by forming a ring around DNA (*35*). Outside the Ku ring, the carboxyl-terminal SAP region of Ku 70 binds DNA through both unstructured amino-terminal lysines and arginines belonging to the NLS and a set of residues at the surface of the SAP globular domain, in a manner similary to what we describe for the lamin−DNA interaction (*36*).

Interactions of LA/C (411−553) Are Impaired by Mutations at R482. Analysis of the solution structure of native LA/C (411−553) showed that mutations causing FPLD are clustered in a solvent-accessible region of LA/C (411−553), which is the main positively charged surface of the Ig-like domain (*12, 13*). These mutations decrease the positively charged character of the surface, but they do not destabilize the structure of the lamin fragment, as shown by circular dichroism and NMR (*12*). Accordingly, it has been suggested that these mutations lower the affinity of LA/C (411−553) for one or several of its biological partners (*12*, *13*). Our experimental data support this hypothesis, since we show here that mutations at arginine 482, the most frequent mutations in FPLD, cause a 5-fold decrease in the affinity of LA/C (411−553) for DNA. It is difficult to predict if mutations occurring in EDMD may affect the binding of LA/C (411−553) to DNA. As these mutations are present in different β-strands, their impact on the structure of loops involved in DNA binding may vary from one mutation to the other.

Work is in progress to investigate the DNA binding of full-length carboxyl-terminal tails of A- and B-type lamins in homologous and heterologous combinations, and to understand how these complexes interact with integral proteins of the inner membrane and chromatin proteins.

ACKNOWLEDGMENT

We thank Drs. Bernard Gilquin, Isabelle Callebaut, Jean-Paul Mornon, François Strauss, Pierre Nicolas, Jean-Michel Camadro, Jean-Jacques Montagne, Erwan Delbarre, Catherine Favreau, Véronique Pizon, and Brigitte Buendia for helpful discussions. We acknowledge Ms. Myriam Barre for the artwork.

REFERENCES

1. Worman, H. J., and Courvalin, J.-C. (2000) *J. Membr. Biol. 177*, 1−11.
2. Stuurman, N., Heins, S., and Aebi, U. (1998) *J. Struct. Biol. 122*, 42−66.
3. McKeon, F. D., Kirschner, M. W., and Caput, D. (1986) *Nature 319*, 463−468.
4. Fisher, D. Z., Chaudhary, N., and Blobel, G. (1986) *Proc. Natl. Acad. Sci. U.S.A. 83*, 6450−6454.
5. Lin, F., and Worman, H. J. (1993) *J. Biol. Chem. 268*, 16321−16326.
6. Worman, H. J., and Courvalin, J.-C. (2002) *Trends Cell Biol. 12*, 591−598.
7. Vigouroux, C., Auclair, M., Dubosclard, E., Pouchelet, M., Capeau, J., Courvalin, J.-C., and Buendia, B. (2001) *J. Cell Sci. 114*, 4459−4468.
8. Fuchs, E., and Weber, K. (1994) *Annu. Rev. Biochem. 63*, 345−382.
9. Glass, C. A., Glass, J. R., Taniura, H., Hasel, K. W., Blevitt, J. M., and Gerace, L. (1993) *EMBO J. 12*, 4413−4424.
10. Taniura, H., Glass, C., and Gerace, L. (1995) *J. Cell Biol. 131*, 33−44.
11. Höger, T. H., Krohne, G., and Kleinschmidt, J. A. (1991) *Exp. Cell Res. 197*, 280−289.
12. Krimm, I., Östlund, C., Gilquin, B., Couprie, J., Hossenlopp, P., Mornon, J.-P., Bonne, G., Courvalin, J.-C., Worman, H. J., and Zinn-Justin, S. (2002) *Structure 10*, 811−823.
13. Dhe-Paganon, S., Werner, E. D., Chi, Y. I., and Shoelson, S. E. (2002) *J. Biol. Chem. 277*, 17381−17384.
14. Rudolph, M. J., and Gergen, J. P. (2001) *Nat. Struct. Biol. 8*, 384−386.
15. Vigouroux, C., Magre, J., Vantyghem, M. C., Bourut, C., Lascols, O., Shackleton, S., Lloyd, D. J., Guerci, B., Padova, G., Valensi, P., Grimaldi, A., Piquemal, R., Touraine, P., Trembath, R. C., and Capeau, J. (2000) *Diabetes 49*, 1958−1962.
16. Duband-Goulet, I., and Courvalin, J.-C. (2000) *Biochemistry 39*, 6483−6488.
17. Goulet, I., Zivanovic, Y., Prunell, A., and Revet, B. (1988) *J. Mol. Biol. 200*, 253−266.
18. Zivanovic, Y., Duband-Goulet, I., Schultz, P., Stofer, E., Oudet, P., and Prunell, A. (1990) *J. Mol. Biol. 214*, 479−495.
19. Sambrook, J., Fritsch, E. F., and Maniatis, T. (1989) *Molecular Cloning: A Laboratory Manual*, 2nd ed., Cold Spring Harbor Laboratory Press, Plainview, NY.
20. Östlund, C., Bonne, G., Schwartz, K., and Worman, H. J. (2001) *J. Cell Sci. 114*, 4435−4445.
21. Laemmli, U. K. (1970) *Nature 227*, 680−685.
22. Duband-Goulet, I., Courvalin, J.-C., and Buendia, B. (1998) *J. Cell Sci. 111*, 1441−1451.
23. Delaglio, F., Grzesiek, S., Vuister, G. W., Zhu, G., Pfeifer, J., and Bax, A. (1995) *J. Biomol. NMR. 6*, 277−293.
24. Shoeman, R. L., and Traub, P. (1990) *J. Biol. Chem. 265*, 9055−9061.
25. Ludérus, M. E. E., de Graaf, A., Mattia, E., den Blaauwen, J. L., and van Driel, R. (1992) *Cell 70*, 949−959.
26. Ludérus, M. E. E., den Blaauwen, J. L., de Smit, O. J. B., Compton, D. A., and van Driel, R. (1994) *Mol. Cell. Biol. 14*, 6297−6305.
27. Burke, B. (1990) *Exp. Cell Res. 186*, 169−176.
28. Glass, J. R., and Gerace, L. (1990) *J. Cell Biol. 111*, 1047−1057.
29. Bennett, C. F., Spector, D. L., and Yeoman, L. C. (1986) *J. Cell Biol. 102*, 600−609.
30. Stuurman, N., Floore, A., Colen, A., de Jong, L., and van Driel, R. (1992) *Exp. Cell Res. 200*, 285−294.
31. Dessev, G. N., Iovcheva-Dessev, C., and Goldman, R. D. (1990) *J. Biol. Chem. 265*, 12636−12641.
32. Broers, J. L., Machiels, B. M., van Eys, G. J., Kuijpers, H. J., Manders, E. M., van Driel, R., and Ramaekers, F. C. (1999) *J. Cell Sci. 112*, 3463−3475.
33. Muralikrishna, B., Dhawan, J., Rangaraj, N., and Parnaik, V. K. (2001) *J. Cell Sci. 114*, 4001−4011.

34. Massagué, J., Blain, S. W., and Lo, R. S. (2000) *Cell 103*, 295−309.
35. Walker, J. R., Corpina, R. A., and Goldberg, J. (2001) *Nature 412*, 607−614.
36. Zhang, Z., Zhu, L., Lin, D., Chen, F., Chen, D. J., and Chen, Y. (2001) *J. Biol. Chem. 276*, 38231−38236.

BI020704G